Accepted Manuscript

Subclinical abnormalities in sarcoplasmic reticulum Ca2+ release promote eccentric myocardial remodeling and pump failure death in response to pressure overload

Simon Sedej, PhD Albrecht Schmidt, MD Marco Denegri, PhD Stefanie Walther, MD Marinko Matovina, Georg Arnstein, MD Eva-Maria Gutschi, Isabella Windhager, MD Senka Ljubojević, PhD Sara Negri, MSc Frank R. Heinzel, MD, PhD Egbert Bisping, MD Marc A. Vos, PhD Carlo Napolitano, MD, PhD Silvia G. Priori, MD, PhD Jens Kockskämper, PhD Burkert Pieske, MD

PII: S0735-1097(13)06194-9

DOI: 10.1016/j.jacc.2013.11.010

Reference: JAC 19623

To appear in: *Journal of the American College of Cardiology*

Received Date: 14 August 2013

Revised Date: 31 October 2013

Accepted Date: 1 November 2013

Please cite this article as: Sedej S, Schmidt A, Denegri M, Walther S, Matovina M, Arnstein G, Gutschi E-M, Windhager I, Ljubojević S, Negri S, Heinzel FR, Bisping E, Vos MA, Napolitano C, Priori SG, Kockskämper J, Pieske B, Subclinical abnormalities in sarcoplasmic reticulum Ca2+ release promote eccentric myocardial remodeling and pump failure death in response to pressure overload, *Journal of the American College of Cardiology* (2013), doi: 10.1016/j.jacc.2013.11.010.

Subclinical abnormalities in sarcoplasmic reticulum Ca^{2+} release promote eccentric myocardial remodeling and pump failure death in response to pressure overload

Running title: Myocardial remodeling in CPVT mice

[1,2]Simon Sedej, PhD, [1]Albrecht Schmidt, MD, [3]Marco Denegri, PhD, [1]Stefanie Walther, MD, [1]Marinko Matovina, [1]Georg Arnstein, MD, [1,2]Eva-Maria Gutschi, [1]Isabella Windhager, MD, [1,2]Senka Ljubojević, PhD, [3]Sara Negri, MSc, [1,2]Frank R. Heinzel, MD, PhD, [1,2]Egbert Bisping, MD, [4]Marc A. Vos, PhD, [3,5]Carlo Napolitano, MD, PhD, [3,5]Silvia G. Priori, MD, PhD, [6]Jens Kockskämper, PhD, [1,2]Burkert Pieske, MD

[1]Department of Cardiology, Medical University of Graz, Austria
[2]Ludwig Boltzmann Institute for Translational Heart Failure Research, Graz, Austria
[3]IRCCS Salvatore Maugeri Foundation and Department of Molecular Medicine, University of Pavia, Italy
[4]Department of Medical Physiology, University Medical Center Utrecht, The Netherlands
[5]Leon H. Charney Division of Cardiology, New York University School of Medicine, USA
[6]Institute of Pharmacology and Clinical Pharmacy, Philipps-University of Marburg, Germany

Funding sources: This work was supported by Start Funding Program of the Medical University of Graz (S.S.), EU FP6 grant LSHM-CT-2005-018802/CONTICA (B.P., S.G.P., M.A.V.). S.G.P. and C.N. are supported by Telethon grants Nos.GGP06007 and GGP11141, CARIPLO pr.2008.2275 and Fondazione Veronesi Award on inherited arrhythmogenic diseases and Fondation Leducq Award to the Alliance for Calmodulin Kinase Signaling in Heart Disease (08CVD01).

Disclosures: None.

Acknowledgements: The authors acknowledge Snjezana Radulovic, Karl-Patrik Kresoja, the staff of the Institute for Biomedical Research (Arno Absenger, Ulrike Fackelmann), Center for Medical Research (ZMF) and Core Facility Molecular Biology for excellent technical assistance. We thank Dr. Gudrun Antoons for critical reading of an earlier version of the manuscript.

Address for correspondence:
Simon Sedej, PhD and Burkert Pieske, MD
Department of Cardiology
Medical University of Graz
Auenbruggerplatz 15
A-8036 Graz
Austria
Tel:+43-316-385-12544
Fax:+43-316-385-13733
e-mail: simon.sedej@medunigraz.at; burkert.pieske@medunigraz.at

Abstract

Objective: We explored whether subclinical alterations of sarcoplasmic reticulum (SR) Ca^{2+} release through cardiac ryanodine receptors (RyR2) aggravate cardiac remodeling in mice carrying a human $RyR2^{R4496C+/-}$ gain-of-function mutation in response to pressure overload.

Background: RyR2 dysfunction causes increased diastolic SR Ca^{2+} release associated with arrhythmias and contractile dysfunction in inherited and acquired cardiac diseases, such as catecholaminergic polymorphic ventricular tachycardia (CPVT) and heart failure (HF).

Methods: Functional and structural properties of wild-type (WT) and CPVT-associated $RyR2^{R4496C+/-}$ hearts were characterized under conditions of pressure overload induced by transverse aortic constriction (TAC).

Results: WT and $RyR2^{R4496C+/-}$ hearts had comparable structural and functional properties at baseline. After TAC, $RyR2^{R4496C+/-}$ hearts responded with eccentric hypertrophy, substantial fibrosis, ventricular dilatation and reduced fractional shortening, ultimately resulting in overt HF. $RyR2^{R4496C+/-}$-TAC cardiomyocytes showed increased incidence of spontaneous SR Ca^{2+} release events, reduced Ca^{2+} transient peak amplitude and SR Ca^{2+} content as well as reduced SR Ca^{2+}-ATPase2a and increased Na^{+}/Ca^{2+}-exchange protein expression. HF phenotype in $RyR2^{R4496C+/-}$-TAC mice was associated with increased mortality due to pump failure, but not tachyarrhythmic events. RyR2-stabilizer K201 markedly reduced Ca^{2+} spark frequency in $RyR2^{R4496C+/-}$-TAC cardiomyocytes. Mini-osmotic pump infusion of K201 prevented deleterious remodeling and improved survival in $RyR2^{R4496C+/-}$-TAC mice.

Conclusions:

The combination of subclinical congenital alteration of SR Ca^{2+} release and pressure overload promotes eccentric remodeling and HF death in $RyR2^{R4496C+/-}$ mice, and pharmacological RyR2 stabilization prevents this deleterious interaction. These findings imply potential clinical relevance for patients with acquired or inherited gain-of-function of RyR2-mediated SR Ca^{2+} release.

Key words: calcium, sarcoplasmic reticulum, remodeling, hypertension, heart failure

Abbreviations and Acronyms

CPVT- catecholaminergic polymorphic ventricular tachycardia
CaMKII- Ca^{2+}/calmodulin-dependent kinase II
ECG- electrocardiogram
HF- heart failure
NCX- Na^{+}/Ca^{2+} exchanger
PLB- phospholamban
RyR2- cardiac ryanodine receptor (type 2)
SERCA2a- sarcoplasmic reticulum Ca^{2+}-ATPase 2a
SR- sarcoplasmic reticulum
TAC- transverse aortic constriction
WT- wild-type

Introduction

Hypertension is the most prevalent cardiovascular risk factor for congestive heart failure (HF) (1). High blood pressure induces left ventricular (LV) hypertrophy as an adaptive compensatory mechanism to reduce LV wall stress in response to hemodynamic overload. Sustained overload induces maladaptive cardiac remodeling, LV dilatation and contractile dysfunction (2), resulting in arrhythmias and HF, a major cause for mortality in the Western world (3).

Pressure overload-induced changes that contribute to cardiac remodeling include an increase in the size of cardiomyocytes, alterations in the extracellular matrix with increased fibrosis (4) and abnormalities of the coronary vasculature (5). Development of hypertrophy and its progression to HF varies considerably between hypertensive individuals, both in the magnitude of LV mass increase and its geometric pattern, such as chamber dilation and wall thickening (6, 7). Yet, the mechanisms that modulate afterload-dependent remodeling processes responsible for these interindividual differences remain incompletely understood (8).

Altered cardiomyocyte Ca^{2+} homeostasis is a central pathophysiological mechanism in hypertrophy and HF (9). Disturbed intracellular Ca^{2+} handling accounts for abnormalities in Ca^{2+} signaling during excitation-contraction coupling (ECC) (10) and also for disturbances in maladaptive gene expression and activation of many Ca^{2+}-dependent hypertrophic signaling pathways (9). Dysfunction of the cardiac ryanodine receptor (RyR2) – the intracellular sarcoplasmic reticulum (SR) Ca^{2+} release channel – is associated with increased spontaneous diastolic SR Ca^{2+} release, delayed afterdepolarizations (DADs) and triggered

activity (11). Consequently, contractile dysfunction and arrhythmias occur in patients with hypertrophy and HF (12), and many of these patients have hypertension as an underlying risk factor or co-morbidity. Increased SR Ca^{2+} leak occurs also in congenital arrhythmia syndromes associated with RyR2 or calsequestrin mutations, such as catecholaminergic polymorphic ventricular tachycardia (CPVT) (13). CPVT is an inherited arrhythmic disorder characterized by sudden cardiac death during physical or emotional stress in the structurally normal heart (13, 14). However, the central role of RyR2 in intracellular Ca^{2+} homeostasis makes it plausible that even subtle abnormalities in RyR2 function may facilitate adverse cardiac remodeling. Therefore, we hypothesized that dysfunctional SR Ca^{2+} release through mutated RyR2 accelerates maladaptive LV remodeling under conditions of pressure overload. We used a knock-in mouse model carrying the $RyR2^{R4496C+/-}$ mutation associated with increased diastolic SR Ca^{2+} leak and CPVT in humans.

Here we show that constitutively abnormal RyR2-mediated SR Ca^{2+} leak promotes myocardial remodeling, including eccentric hypertrophy, dilatation and contractile dysfunction, and increases mortality due to pump failure in $RyR2^{R4496C+/-}$ mice under pressure overload. Conversely, pharmacological stabilization of SR Ca^{2+} release by K201 ameliorates the development of HF and preserves systolic function.

Methods

An expanded version of the Methods section can be found in the Online Appendix. Heterozygous $RyR2^{R4496C+/-}$ knock-in mice (R4496C) and their wild-type (WT) littermates underwent surgery without (Sham) or with transverse aortic constriction (TAC). Dimensions and function of the LV were assessed by transthoracic echocardiography (micro-imaging system Vevo770®, 30-MHz transducer, VisualSonics, Canada). Arrhythmias were continuously monitored by ECG radiotelemetry (DSI, USA). RyR2-stabilizing agent K201 was administered via mini-osmotic pumps (Alzet, USA). Cardiomyocytes were isolated 1

week post-surgery as described previously (15). $[Ca^{2+}]_i$ measurements were acquired in line-scan mode by a confocal microscope (LSM 5 Pascal, Zeiss, Germany) using the solutions, recording protocols and analysis described previously (16). Data are shown as mean±S.E.M.. Statistical differences between groups were considered significant when $P<0.05$.

Results

Additional Figures of the Results section can be found in the Online Appendix.

Myocardial remodeling and fibrosis

Increased afterload on the LV was induced by TAC (Fig. 1A). In WT and R4496C mice, 1 week of TAC induced similar degrees of cardiac hypertrophy as defined by an increased heart weight-to-tibia length (Fig. 1B). Three weeks post-TAC, however, relative heart weight had increased significantly more in R4496C-TAC hearts as compared to WT-TAC hearts (11.3±0.7 mg/mm vs. 9.4±0.3 mg/mm, $P<0.05$, respectively, Fig. 1B). R4496C-TAC mice had elevated lung weight-to-tibia length ratio (5.7±0.6 mg/mm, $P<0.05$) compared with WT-TAC mice (3.9±0.3 mg/mm, Fig. 1C). Increased relative heart weight correlated with induction of the hypertrophic gene program (Figs. 1E-F), and activation of hypertrophic genes was more prominent in R4496C-TAC hearts. Accelerated remodeling of R4496C-TAC hearts was associated with more fibrosis ($P<0.05$ versus WT-TAC, Figs. 1A, D) and increased myocyte length/width ratio in isolated R4496C-TAC cardiomyocytes (Fig. 1G).

Accelerated progression from hypertrophy to HF

R4496C-TAC mice underwent progressive LV chamber dilatation that started within the first week after TAC (Figs. 2A-B). In contrast, WT-TAC mice effectively compensated pressure overload at 1 week post-TAC with moderate increases in LVEDD 3 weeks post-TAC. Increased dilatation in conjunction with smaller LV wall thickness suggested that R4496C-TAC hearts underwent accelerated transition from load-induced hypertrophy to HF (Fig. 2B). Fractional shortening declined more in R4496C-TAC hearts at 1 week (WT-TAC:-

6.2±2.4%, R4496C-TAC:-18.1±2.3%, $P<0.05$) and 3-weeks post-TAC (WT-TAC:-14.3±1.9%, R4496C-TAC:-23.9±1.7, $P<0.05$, Fig. 2C). WT hearts responded with a significant increase in the relative wall thickness to pressure overload. This physiological response was absent in R4496C-TAC mice ($P<0.05$ versus WT-TAC, Fig. 2D). Eccentric LV remodeling in R4496C-TAC mice was associated with premature death: only 36% of animals were alive after 6 weeks of TAC compared to 74% survival in WT-TAC mice ($P<0.05$, Fig. 2E).

Impaired survival due to pump failure death in R4496C-TAC mice

Susceptibility to catecholamine-induced tachyarrhythmias and sudden cardiac death (17) could explain increased mortality in R4496C-TAC mice. ECG transmitters were implanted in a subset of R4496C-TAC mice (N=11) to allow continuous recording of ambulatory ECG waveforms. All of the R4496C-TAC mice (11/11), however, had sinus rhythm followed by progressing sinus bradycardia and atrio-ventricular conduction block III, and ultimately died from pump failure (Figs. 3A-B). In another set of experiments, we examined whether R4496C-TAC mice were vulnerable to CPVT under conditions that resemble those eliciting tachyarrhythmias in CPVT patients (14). Epinephrine and RyR2-agonist caffeine administration increased heart rate and induced sustained bidirectional ventricular tachycardia in 100% (6/6) of the R4496C-TAC survivors 1 week post-TAC (Fig. 3C). Persistent bidirectional ventricular tachycardia induced by epinephrine/caffeine did not deteriorate into bradycardia followed by asystole, but subsided within 30 min and failed to induce sudden cardiac death in 100% (6/6) of the R4496C-TAC mice (Fig. 3C). These mice developed progressive sinus bradycardia a few days later and died thereafter due to pump failure.

Increased SR Ca^{2+} leak in R4496C-TAC mice

We investigated whether pressure overload increases RyR2-mediated SR Ca^{2+} leak measured as Ca^{2+} sparks (Fig. 4A). Ca^{2+} spark frequency at matched SR Ca^{2+} load (Fig. 4B) revealed a pronounced increase in SR Ca^{2+} leak in R4496C-sham as compared to WT-sham (173.6±20.9 $pL^{-1}s^{-1}$ and 102.2±9.7 $pL^{-1}s^{-1}$, respectively, $P<0.05$, Fig. 4C). Ca^{2+} spark frequency at matched SR Ca^{2+} load was largely increased in R4496C-TAC cardiomyocytes (332.7±42.9 $pL^{-1}s^{-1}$, $P<0.05$) versus WT-TAC (190.1±27 $pL^{-1}s^{-1}$, Fig. 4C).

Impaired global Ca^{2+} homeostasis

At baseline, sham-operated WT and R4496C cardiomyocytes displayed similar Ca^{2+} transients (Suppl. Figs. 1A-D). However, the peak of the caffeine-induced Ca^{2+} transient was diminished in R4496C-sham vs. WT-Sham cardiomyocytes ($P<0.05$, Suppl. Fig. 1E). At 1 week post-TAC, R4496C-TAC myocytes displayed significantly reduced peak amplitudes of Ca^{2+} transients, prolonged $[Ca^{2+}]_i$ transient decline and further reduced SR Ca^{2+} content (Suppl. Figs. 1B-C and E, all $P<0.05$ vs. WT-TAC).

Altered expression and phosphorylation of Ca^{2+} regulatory proteins

Phosphorylation of RyR2 at Ser2808 and at Ser2814 and also at Ser16 of PLB was unaltered in all groups (Suppl. Figs. 2A-B). However, phosphorylation of PLB at Thr17 was significantly decreased in R4496C (Sham and TAC) mice (Suppl. Fig. 2B). SERCA2a levels were reduced in both WT-TAC and R4496C-TAC hearts compared to WT-Sham (Suppl. Fig. 2C, $P<0.05$). In contrast, NCX expression was significantly increased in R4496C-TAC mice only, but unchanged in WT-sham hearts (Suppl. Fig. 2C).

Altered differential expression and phosphorylation of CaMKII, calcineurin and protein phosphatase 1

Under baseline conditions, overall CaMKII expression and phosphorylation was similar, but the expression of CaMKIIγ was significantly higher in R4496C vs. WT (Suppl. Fig. 2D). After 1 week of TAC, CaMKII expression and phosphorylation were significantly

increased in both, WT and R4496C hearts (Suppl. Fig. 2D). However, this increase was significantly higher in R4496C-TAC hearts (P<0.05 vs. WT-TAC). Interestingly, the overall increase in CaMKII after TAC was related to differential regulation of its isoforms γ and δ: while CaMKIIγ was largely increased after TAC in WT, CaMKIIδ remained unchanged; in contrast, the smaller increase in CaMKIIγ in R4496C was associated with a parallel increase in CaMKIIδ. Calcineurin protein levels significantly increased with TAC in WT hearts, but were already elevated in R4496C hearts at baseline with no further change after TAC (Suppl. Fig. 2E). Protein phosphatase 1 levels were not affected by TAC, but were upregulated in both R4496C groups (Suppl. Fig. 2E).

K201 ameliorated the progression of HF and improved survival in R4496C-TAC mice

Infusion of K201 resulted in a mean K201 plasma concentration of 69.1±10.8 ng/ml (N=6). After TAC, K201 prevented LV dilatation (LVESD, Fig. 5A), prevented the decline in fractional shortening (1 week:+6.6±2.6%, 3 weeks:+7.9±2.6%, both P<0.05 versus control, Fig. 5B), restored an increase in the relative wall thickness (Fig. 7C) and largely prevented the accelerated transition from concentric to eccentric remodeling and LV dilatation in R4496C-TAC mice (LVEDD, Fig. 5D). K201 treatment normalized survival over 6 weeks after TAC (Fig. 5E). At 6 weeks, 83% of K201-treated R4496C-TAC mice were alive as compared to 31% treated with the vehicle (P<0.05).

K201 prevented the spontaneous SR Ca^{2+} release in R4496C-TAC mice

To test whether the beneficial effect of K201 is related to a reduction in SR Ca^{2+} leak in R4496C-TAC cardiomyocytes, we assessed the effect of 300 nmol/L K201 and 1 □mol/L dantrolene (RyR2 stabilizers) and 1 □mol/L KN-93 (CaMKII inhibitor) on Ca^{2+} spark frequency and global Ca^{2+} homeostasis. K201 and dantrolene markedly reduced the increase in Ca^{2+} spark frequency at matched SR Ca^{2+} load in R4496C-TAC and WT-TAC cells as well as R4496C-Sham cells (Figs. 6A-B). The RyR2 stabilizing effect was more pronounced in

the presence of K201 than dantrolene (Figs. 6A-B). None of the RyR2-channel stabilizers changed the peak Ca^{2+} transient amplitude (Fig. 6C) and kinetics (not shown) in TAC groups. However, the peak of the caffeine-induced Ca^{2+} transient was increased with K201 and dantrolene treatment in WT-TAC and R4496C-TAC cells (Fig. 6D). In contrast to K201 and dantrolene administration, KN-93 treatment did not significantly alter the Ca^{2+} spark frequency and global Ca^{2+} homeostasis in any of the groups studied (Figs. 6A-D).

Discussion

Here we demonstrated that the CPVT-associated $RyR2^{R4496C+/-}$ gain-of-function mutation promotes adverse structural and functional myocardial remodeling, HF and pump failure death in response to pressure overload. RyR2 stabilization by K201 attenuates the SR Ca^{2+} leak, ameliorates the TAC-induced transition from hypertrophy to HF and improves survival of $RyR2^{R4496C+/-}$ mice.

Ca^{2+} dysregulation and adverse remodeling

Increased SR Ca^{2+} leak via RyR2 channels and reduced Ca^{2+} uptake by SERCA2a contribute to reduced SR Ca^{2+} content and increased diastolic Ca^{2+} concentration in hypertrophy and HF (18). $RyR2^{R4496C+/-}$ knock-in mice display increased SR Ca^{2+} release (15) in structurally normal hearts, resulting in increased diastolic Ca^{2+} concentration and catecholamine-induced bidirectional tachycardias and ventricular fibrillation (14) similar to humans (13). Our results show that the combination of pressure overload and dysregulated SR Ca^{2+} release through mutated $RyR2^{R4496C+/-}$ channel promotes rapid cardiac remodeling. A remarkable shift in the pattern of hypertrophic remodeling related to increased SR Ca^{2+} leak was reflected in altered gene expression, increased fibrosis and relative heart weight, eccentric hypertrophy, LV dilatation and dysfunction, which progressed into overt HF. The involvement of RyR2-mediated SR Ca^{2+} release for the development of pressure overload-induced hypertrophy has been recently demonstrated in $RyR2^{R176Q+/-}$ knock-in mice

(19) and RyR2$^{+/-}$-deficient mice (20). While reduced SR Ca^{2+} release was associated with less concentric hypertrophy and fibrosis after 3 weeks of TAC (20), elevated SR Ca^{2+} release via RyR2$^{R176Q+/-}$ mutated channels enhanced the hypertrophic response accompanied by impaired diastolic and systolic function, and LV dilation by activation of the calcineurin/NFAT signaling pathway in response to aortic constriction (19). Our study extends these findings and provides evidence that the congenital RyR2 dysfunction promotes adverse myocardial remodeling, including aggravation of RyR2-mediated SR Ca^{2+} leak and altered intracellular Ca^{2+} handling, both of which may contribute to the pronounced shift in phenotypic remodeling during pressure overload.

During the development of myocardial hypertrophy and before the transition to HF, the contribution of SERCA2a to Ca^{2+} removal is reduced and already shifted in favour of the NCX and defective Ca^{2+} uptake into the SR is partially compensated for by increased NCX expression (21). In R4496C-TAC mice, this shift was reflected in reduced SR Ca^{2+} content, reduced peak amplitude of the Ca^{2+} transient and prolonged $[Ca^{2+}]_i$ transient decline, indicating decreased contractility and impaired relaxation, respectively. Reduced SR Ca^{2+} content, a major cause for contractile dysfunction in R4496C-TAC hearts, was associated with the reduced SERCA2a-dependent Ca^{2+} removal, increased expression of NCX, and increased Ca^{2+} spark frequency. These findings provide compelling evidence for the pathophysiological relevance of dysfunctional SR Ca^{2+} release in the dysregulation of SR Ca^{2+} handling, which, in turn, provides the basis for the cardiomyocyte malfunctioning associated with the development of pressure overload-induced hypertrophy.

Increased expression and activity of CaMKII in R4496C hearts at 1 week after aortic constriction suggest that an early development of HF phenotype in R4496C-TAC mice is, at least partially, attributed to the activation of CaMKII-dependent hypertrophy pathways. This contrasts with the study by van Oort *et al.* (19), in which the authors ruled out the possible

role of elevated SR Ca^{2+} leak in the activation of CaMKII-dependent hypertrophy signaling. Recent studies demonstrated that CaMKIIδ is required for alterations in the expression of Ca^{2+} regulatory proteins during the development of pressure overload-induced HF (22). Conversely, CaMKIIδ deletion protects from adverse remodeling after pressure overload (23) and progression from pressure-overload hypertrophy to HF (22). A disparity in the expression between CaMKIIγ and CaMKIIδ isoform in R4496C-TAC hearts supports the hypothesis that increased expression of CaMKIIδ provoked early onset of adverse myocardial remodeling. Upregulation of $CaMKII\delta_c$ also contributes to abnormal Ca^{2+} handling and increased mortality in R4496C mice (24). Notably, increased levels of CaMKII did not affect the phosphorylation of RyR2 and PLB in R4496C mice likely due to increased PP1 levels. Hence, our findings suggest that maladaptive CaMKII signaling was affecting structural myocardial remodeling rather than functionally interfering with Ca^{2+} cycling. In support of this hypothesis, we found that CaMKII inhibition with KN-93 did not attenuate Ca^{2+} spark frequency and interfere with ECC in the absence of catecholaminergic stimulation in R4496C-TAC cardiomyocytes as described previously (17). Previous studies emphasize the importance of CaMKII-mediated phosphorylation of RyR2 in the progression of (non-ischemic form) of HF in both humans (12) and TAC mice (25, 26). However, our results suggest minor role of the CaMKII-mediated phosphorylation of RyR2 at Ser2814 on aberrant SR Ca^{2+} release via RyR2 and *in vivo* cardiac dysfunction. This discrepancy may be related to different time points at which the phosphorylation of RyR2 at Ser2814 was assessed or the severity of cardiac decompensation (25, 26). In agreement with the study by van Oort *et al*. (19), we found increased expression levels of calcineurin in pressure overload-imposed R4496C hearts (but also in WT), indicating the activation of the Ca^{2+}-dependent calcineurin/NFAT hypertrophic signaling pathway.

Increased mortality and mode of death

Our study shows, for the first time, that pressure overload impaired survival of R4496C mice due to pump failure rather than ventricular arrhythmias. Given that acute adrenergic stimulation predisposes R4496C mice to CPVT and ventricular fibrillation (27), we anticipated that increased propensity for ventricular arrhythmia was a major cause for increased mortality in R4496C mice imposed to pressure overload. However, even though R4496C-TAC cardiomyocytes exhibited an increased arrhythmogenic potential *in vitro*, including increased SR Ca^{2+} leak, reduced SERCA2a-dependent Ca^{2+} removal, and increased expression of NCX, ventricular arrhythmias and sudden cardiac death were not observed *in vivo* in R4496C mice under pressure overload. Several reasons may account for this phenomenon, including reduced SR Ca^{2+} content and □-adrenergic responsiveness and the absence of CaMKII-dependent phosphorylation of RyR2, which has been shown to be required for arrhythmogenic events leading to sudden cardiac death (24, 25). Triggered activity was effectively compensated by reduced SR Ca^{2+} load in the R4496C-TAC myocytes, such that the diastolic SR Ca^{2+} leak was insufficient to produce triggered activity unless SR Ca^{2+} content was increased (28). In response to □-adrenergic stimulation, however, the R4496C mutation results in largely increased SR Ca^{2+} leak and SR Ca^{2+} content due to increased CaMKII site-dependent RyR2 phosphorylation and increased SR Ca^{2+} reuptake, respectively (17). This has been related to an increased propensity to DAD-mediated triggered activity underlying ventricular tachyarrhythmia (27), which could also be elicited in our R4496C-TAC hearts upon catecholamine stimulation. Faster heart rate and SR Ca^{2+} uptake during adrenergic stimulation increases SR Ca^{2+} load and induces subsequent Ca^{2+} waves followed by DAD-mediated triggered beats in ventricular cardiomyocytes harboring RyR2 mutations (27, 29). Notably, triggered activity in R4496C cardiomyocytes occurs also upon increasing SR Ca^{2+} content in the absence of adrenergic stimulation (15).

These findings jointly highlight the importance of elevated SR Ca^{2+} content as a principal trigger in the CPVT arrhythmogenesis.

Effects of pharmacological RyR2 stabilization on adverse remodeling

Prevention of excessive diastolic RyR2-mediated SR Ca^{2+} release with K201 suppresses SR Ca^{2+} leak by stabilizing defective RyR2 gating (30) and improves cardiac and skeletal muscle function in HF (31). Thus, RyR2 stabilizers have been proposed as a therapeutic strategy in patients with HF (31, 32). We found that the correction of dysfunctional Ca^{2+} release by chronic administration of K201 (plasma concentration ~160 nmol/L) ameliorated the development of eccentric dilatation, improved LV systolic function and, most importantly, improved survival of R4496C-TAC mice. The evidence that K201 decelerates the progression of HF in CPVT mice after pressure overload extends previous findings, which demonstrate that K201 improves contractile function in tissue from end-stage human failing hearts (33) and delays the progression of ventricular remodeling and dysfunction by inhibiting the SR Ca^{2+} leak (31). Our *in vitro* experiments demonstrated that K201 (at 300 nmol/L) as well as dantrolene abolished acquired as well as congenital RyR2-mediated SR Ca^{2+} leak to almost normal levels. Three findings confirm that K201 reduces RyR2 open probability in WT-TAC and R4496C cells. Firstly, K201 attenuated Ca^{2+} spark frequency in all “diseased” groups. Secondly, K201 decreased systolic $[Ca^{2+}]_i$ in R4496C-Sham cells. Thirdly, in WT- and R4496C-TAC cardiomyocytes, K201 (and dantrolene) increased the SR Ca^{2+} content and reduced fractional release. This is consistent with our recent study (15), in which we demonstrated that the dominant effect of K201 is RyR2 stabilization associated with reduced SR Ca^{2+} leak in R4496C cells under conditions of similar and/or increased SR Ca^{2+} content. Interestingly, K201 prevented SR Ca^{2+} leak more effectively than dantrolene, implying that differences in the mode of interdomain interaction in those different regions, to which K201 and dantrolene bind, may result in the observed differences in their RyR2-

stabilizing efficacy (34). Notably, K201 and dantrolene treatment did not alter Ca^{2+} spark frequency and intracellular Ca^{2+} handling in WT-Sham cells, suggesting that both RyR2 stabilizers may be effective only in repairing defective inter-domain interactions of the RyR2. Our study showed that the R4496C-TAC model has a much more complex pathophysiology than the non-TAC CPVT model. Therefore, the finding that K201 does not seem to prevent arrhythmias in R4496C mice without TAC (27) may simply mean that K201 acts on different pathways than to eliminate store overload-induced Ca^{2+} release (which is probably the reason for arrhythmias in CPVT). Taken together, we found that K201 and dantrolene suppressed SR Ca^{2+} leak by stabilizing defective RyR2 gating, confirming that destabilization of RyR2 and consequent SR Ca^{2+} leak plays a pivotal role in TAC-induced remodeling.

Potential clinical relevance

Our finding that increased diastolic SR Ca^{2+} release is causally involved in the accelerated pathogenesis of pressure overload-induced HF has important clinical implications. First, our study suggests that CPVT patients (with RyR2 mutations) that eventually develop hypertension may be particularly vulnerable to the development of eccentric hypertrophy and HF. Thus, it is possible that CPVT patients present a “latent” substrate for mechanical dysfunction that becomes overt with appropriate triggers. This concept is corroborated by evidence for an atypical form of cardiomyopathy reported in association with some RyR2 mutations (35, 36). Interestingly, genome-wide association studies demonstrate that some RyR2 variants (single nucleotide polymorphisms) increase susceptibility to hypertension (37), indicating that aberrant RyR2 function could represent an underlying pathogenic risk factor in heart disease. Second, acquired imbalances of SR Ca^{2+} release are common findings in patients with hypertrophy and HF. Many of these patients have hypertension as an underlying risk factor or co-morbidity. This unfavorable combination may underlie rapid progression of myocardial remodeling in some of these patients and may

partially explain interindividual differences in the pattern of remodeling (eccentric vs. concentric hypertrophy).

In summary, in conditions of pressure overload, the gain-of-function R4496C mutation in RyR2 accelerates the development of congestive HF and increases mortality due to pump failure rather than tachyarrhythmias. K201 attenuates the development of HF and improves survival in R4496C-TAC mice. We suggest that RyR2-mediated SR Ca^{2+} leak contributes to the myocardial remodeling under pressure overload. Our study proposes that RyR2 stabilizers may provide a novel and rational approach to effectively combat hypertrophy and development of HF in patients with hypertension and acquired or congenital increased RyR2-mediated Ca^{2+} leak.

References

1. Levy D, Larson MG, Vasan RS, Kannel WB, Ho KK. The progression from hypertension to congestive heart failure. JAMA. 1996;275:1557-62.

2. Chien KR. Stress pathways and heart failure. Cell. 1999;98:555-8.

3. McMurray JJ, Pfeffer MA. Heart failure. Lancet. 2005;365:1877-89.

4. Berk BC, Fujiwara K, Lehoux S. ECM remodeling in hypertensive heart disease. J Clin Invest. 2007;117:568-75.

5. Bishop SP, Powell PC, Hasebe N, *et al*. Coronary vascular morphology in pressure-overload left ventricular hypertrophy. J Mol Cell Cardiol. 1996;28:141-54.

6. Ganau A, Devereux RB, Roman MJ, *et al*. Patterns of left ventricular hypertrophy and geometric remodeling in essential hypertension. J Am Coll Cardiol. 1992;19:1550-8.

7. Sehgal S, Drazner MH. Left ventricular geometry: Does shape matter? Am Heart J. 2007;153:153-5.

8. Drazner MH. The progression of hypertensive heart disease. Circulation. 2011;123:327-34.

9. Berridge MJ, Bootman MD, Roderick HL. Calcium signalling: Dynamics, homeostasis and remodelling. Nat Rev Mol Cell Biol. 2003;4:517-29.

10. Pieske B, Maier LS, Bers DM, Hasenfuss G. Ca2+ handling and sarcoplasmic reticulum Ca2+ content in isolated failing and nonfailing human myocardium. Circ Res. 1999;85:38-46.

11. Bers DM. Cardiac excitation-contraction coupling. Nature. 2002;415:198-205.

12. Fischer TH, Herting J, Tirilomis T, *et al*. Ca2+/calmodulin-dependent protein kinase II and protein kinase A differentially regulate sarcoplasmic reticulum Ca2+ leak in human cardiac pathology. Circulation. 2013;128:970-81.

13. Priori SG, Napolitano C, Memmi M, *et al*. Clinical and molecular characterization of patients with catecholaminergic polymorphic ventricular tachycardia. Circulation. 2002;106:69-74.

14. Cerrone M, Colombi B, Santoro M, *et al.* Bidirectional ventricular tachycardia and fibrillation elicited in a knock-in mouse model carrier of a mutation in the cardiac ryanodine receptor. Circ Res. 2005;96:e77-82.

15. Sedej S, Heinzel FR, Walther S, *et al.* Na+-dependent SR Ca2+ overload induces arrhythmogenic events in mouse cardiomyocytes with a human CPVT mutation. Cardiovasc Res. 2010;87:50-9.

16. Sacherer M, Sedej S, Wakula P, *et al.* JTV519 (K201) reduces sarcoplasmic reticulum ca(2+) leak and improves diastolic function in vitro in ouabain-induced cellular ca(2+) overload in murine and human non-failing myocardium. Br J Pharmacol. 2012.

17. Liu N, Ruan Y, Denegri M, *et al.* Calmodulin kinase II inhibition prevents arrhythmias in RyR2(R4496C+/-) mice with catecholaminergic polymorphic ventricular tachycardia. J Mol Cell Cardiol. 2011;50:214-22.

18. Bers DM, Eisner DA, Valdivia HH. Sarcoplasmic reticulum Ca2+ and heart failure: Roles of diastolic leak and Ca2+ transport. Circ Res. 2003;93:487-90.

19. van Oort RJ, Respress JL, Li N, *et al.* Accelerated development of pressure overload-induced cardiac hypertrophy and dysfunction in an RyR2-R176Q knockin mouse model. Hypertension. 2010;55:932-8.

20. Zou Y, Liang Y, Gong H, *et al.* Ryanodine receptor type 2 is required for the development of pressure overload-induced cardiac hypertrophy. Hypertension. 2011;58:1099-110.

21. Hasenfuss G. Alterations of calcium-regulatory proteins in heart failure. Cardiovasc Res. 1998;37:279-89.

22. Ling H, Zhang T, Pereira L, *et al.* Requirement for Ca2+/calmodulin-dependent kinase II in the transition from pressure overload-induced cardiac hypertrophy to heart failure in mice. J Clin Invest. 2009;119:1230-40.

23. Backs J, Backs T, Neef S, *et al*. The delta isoform of CaM kinase II is required for pathological cardiac hypertrophy and remodeling after pressure overload. Proc Natl Acad Sci U S A. 2009;106:2342-7.

24. Dybkova N, Sedej S, Napolitano C, *et al.* Overexpression of CaMKIIdeltac in RyR2R4496C+/- knock-in mice leads to altered intracellular Ca2+ handling and increased mortality. J Am Coll Cardiol. 2011;57:469-79.

25. van Oort RJ, McCauley MD, Dixit SS, *et al*. Ryanodine receptor phosphorylation by calcium/calmodulin-dependent protein kinase II promotes life-threatening ventricular arrhythmias in mice with heart failure. Circulation. 2010;122:2669-79.

26. Respress JL, van Oort RJ, Li N, *et al*. Role of RyR2 phosphorylation at S2814 during heart failure progression. Circ Res. 2012;110:1474-83.

27. Liu N, Colombi B, Memmi M, *et al.* Arrhythmogenesis in catecholaminergic polymorphic ventricular tachycardia: Insights from a RyR2 R4496C knock-in mouse model. Circ Res. 2006;99:292-8.

28. Kashimura T, Briston SJ, Trafford AW, *et al*. In the RyR2(R4496C) mouse model of CPVT, beta-adrenergic stimulation induces ca waves by increasing SR ca content and not by decreasing the threshold for ca waves. Circ Res. 2010;107:1483-9.

29. Kannankeril PJ, Mitchell BM, Goonasekera SA, *et al.* Mice with the R176Q cardiac ryanodine receptor mutation exhibit catecholamine-induced ventricular tachycardia and cardiomyopathy. Proc Natl Acad Sci U S A. 2006;103:12179-84.

30. Tateishi H, Yano M, Mochizuki M, *et al*. Defective domain-domain interactions within the ryanodine receptor as a critical cause of diastolic Ca2+ leak in failing hearts. Cardiovasc Res. 2009;81:536-45.

31. Wehrens XH, Lehnart SE, Reiken S, *et al*. Enhancing calstabin binding to ryanodine receptors improves cardiac and skeletal muscle function in heart failure. Proc Natl Acad Sci U S A. 2005;102:9607-12.

32. Yano M, Kobayashi S, Kohno M, *et al*. FKBP12.6-mediated stabilization of calcium-release channel (ryanodine receptor) as a novel therapeutic strategy against heart failure. Circulation. 2003;107:477-84.

33. Toischer K, Lehnart SE, Tenderich G, *et al*. K201 improves aspects of the contractile performance of human failing myocardium via reduction in Ca2+ leak from the sarcoplasmic reticulum. Basic Res Cardiol. 2010;105:279-87.

34. Suetomi T, Yano M, Uchinoumi H, *et al*. Mutation-linked defective interdomain interactions within ryanodine receptor cause aberrant ca(2)release leading to catecholaminergic polymorphic ventricular tachycardia. Circulation. 2011;124:682-94.

35. Chiu C, Tebo M, Ingles J, *et al*. Genetic screening of calcium regulation genes in familial hypertrophic cardiomyopathy. J Mol Cell Cardiol. 2007;43:337-43.

36. Milting H, Lukas N, Klauke B, *et al*. Composite polymorphisms in the ryanodine receptor 2 gene associated with arrhythmogenic right ventricular cardiomyopathy. Cardiovasc Res. 2006;71:496-505.

37. Wellcome Trust Case Control Consortium, Australo-Anglo-American Spondylitis Consortium (TASC), Burton PR, *et al*. Association scan of 14,500 nonsynonymous SNPs in four diseases identifies autoimmunity variants. Nat Genet. 2007;39:1329-37.

Figure Legends

Figure 1: Myocardial remodeling and fibrosis

(A) Photomicrographs of hearts (3 weeks post-surgery, top); Hematoxylin/eosin- (middle) and picrosirius red-stained heart sections (bottom). **(B)** Heart weight/tibia length ratio (HW/TL). **(C)** Lung weight/tibia length ratio (LW/TL, N=13-24 mice). **(D)** Collagen content (N=8-10 mice). **(E)** Messenger RNA levels of □-myosin heavy chain (Myh7b), **(F)** brain natriuretic peptide (Nppb) (N=6-8 mice). **(G)** Cell length-to-width ratio. Numbers in bars indicate the number of cardiomyocytes measured (N=5 mice/group). TAC1 and TAC3 indicate 1 and 3 weeks post-TAC, respectively. $^{\cdot}P<0.05$ versus sham, $^{\#}P<0.05$ versus WT-TAC.

Figure 2: Cardiac remodeling, function and survival

(A) Echocardiographic M-mode images of the left ventricle (LV). **(B)** Sum of intraventricular septum (IVS) and posterior wall (PW) thickness plotted versus left ventricular end-diastolic diameter (LVEDD) as an indicator for concentric vs. dilative remodeling. R4496C-TAC mice (N=12-14) displayed accelerated transition from concentric hypertrophy to dilatation vs. WT-TAC mice (N=15-21). **(C)** Systolic function indicated by fractional shortening (echocardiography) over time. **(D)** Relative LV wall thickness, indicating eccentric vs. concentric remodeling in R4496C-TAC and WT-TAC mice, respectively. **(E)** Kaplan-Meier survival curve. Number in parenthesis indicates the number of animals tested in each group. Dotted line represents 3 weeks post-TAC. $^{\cdot}P<0.05$ versus sham, $^{\#}P<0.05$ versus WT-TAC.

Figure 3: Increased mortality due to pump failure death in R4496C-TAC mice

A. Progressive decline in heart rate (HR) after TAC (the last 16 hours before death shown by the inset). **(B_1-B_4)** Original ECG recordings from a R4496C-TAC mouse. Note that sinus rhythm was followed by progressing sinus bradycardia and atrio-ventricular conduction block III. **(C)** Caffeine/epinephrine co-injection (arrow) increased the HR and evoked non-lethal CPVT episodes in R4496C-TAC mice (N=6). Insets show typical ECG recordings at various time points.

Figure 4: Ca^{2+} spark frequency

(A) Original confocal line-scan images. **(B)** Ca^{2+} spark frequency as a function of SR Ca^{2+} load (each symbol represents one cell). **(C)** Increased Ca^{2+} spark frequency at matched SR Ca^{2+} content (box in B) showed elevated SR Ca^{2+} leak in R4496C-TAC. Numbers in bars indicate the number of cells tested 1 week post-surgery (TAC1). $^{\cdot}P<0.05$ versus respective Sham, $^{\#}P<0.05$ versus WT-TAC.

Figure 5: K201 effect on R4496C-TAC hearts

(A) K201 decreased LV end-systolic diameter (LVESD), **(B)** improved fractional shortening, **(C)** increased LV wall thickness 1 week and 3 weeks post-TAC in R4496C-TAC mice versus vehicle-treated R4496C-TAC mice. **(D)** K201 ameliorated the development of TAC-induced HF in R4496C mice (N=11) compared to vehicle-treated R4496C-TAC mice (N=5-6). **(E)** Kaplan-Meier survival curve. Numbers in parenthesis indicate the number of animals tested before and after 3 weeks TAC (dotted line). For comparison, baseline data from WT-TAC and R4496C-TAC mice are included (Figure 2). $^{\cdot}P<0.05$ versus K201-treated R4496C-TAC mice. $^{\S}P<0.05$ versus vehicle-treated R4496C-TAC mice.

Figure 6: K201 prevents SR Ca^{2+} leak in R4496C cardiomyocytes

(A_{1-3}) Ca^{2+} spark frequency as a function of SR Ca^{2+} content (each symbol represents one cell) in K201-, dantrolene- and KN-93-treated cells, respectively. **(B)** Ca^{2+} spark frequency matched for SR Ca^{2+} load in K201-, dantrolene- and KN-93-treated cardiomyocytes. **(C)** Ca^{2+} transient peak amplitude, **(D)** SR $[Ca^{2+}]$ content. N=10-45 cells per treatment group were tested 1 week after Sham/TAC. $^{\cdot}P<0.05$ versus respective WT-Sham treatment group, $^{\#}P<0.05$ versus respective WT-TAC treatment group, $^{\S}P<0.05$ versus respective control group (white bars), $^{\ddagger}P<0.05$ versus respective K201-treated group, $^{\&}P<0.05$ versus respective R4496C-Sham.

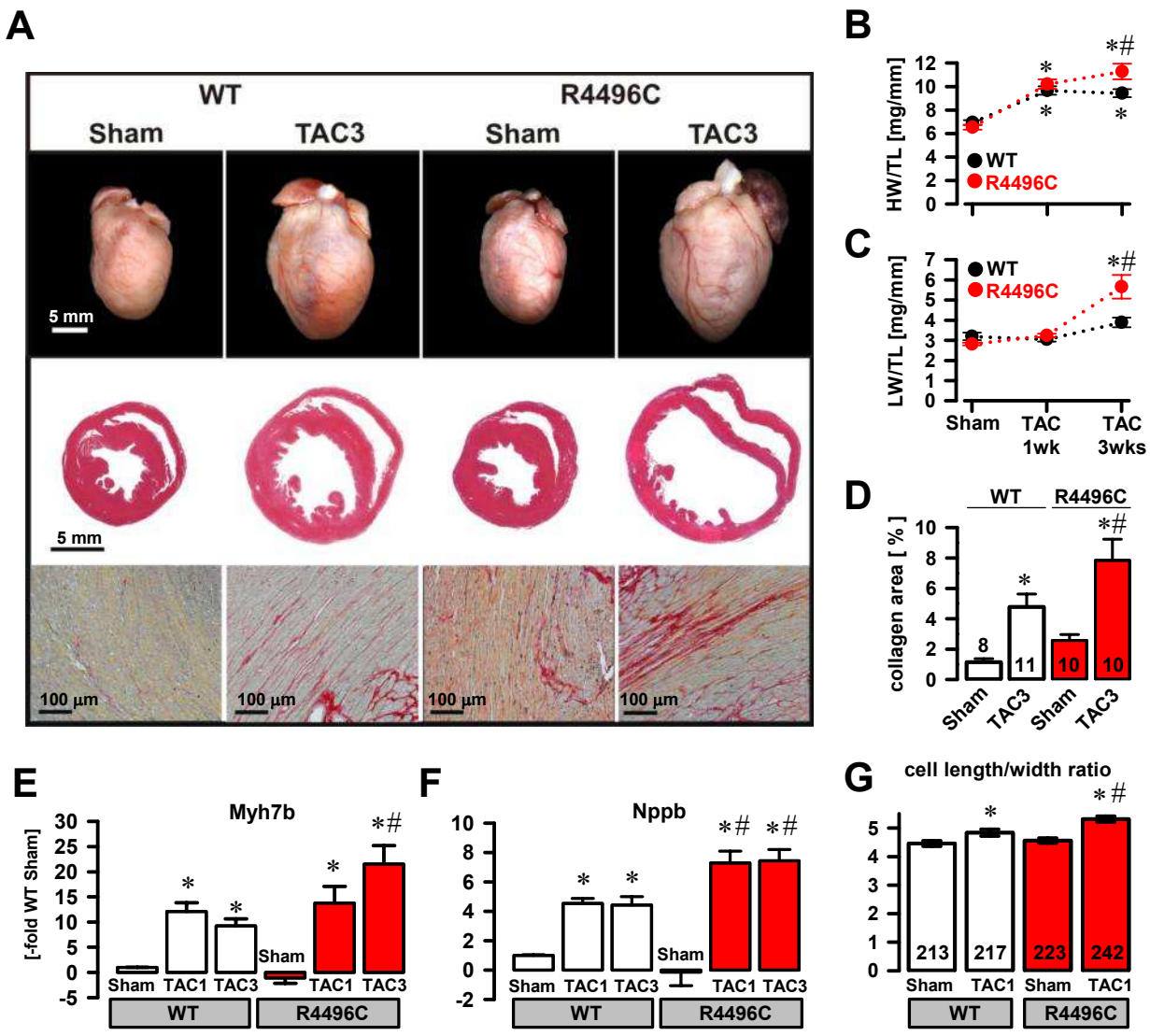
A
WT
R4496C
Sham
TAC3
Sham
TAC3
5 mm
5 mm
100 µm
100 µm
100 µm
100 µm
B
HW/TL [mg/mm]
WT
R4496C
C
LW/TL [mg/mm]
WT
R4496C
Sham
TAC 1wk
TAC 3wks
D
WT
R4496C
collagen area [%]
8
11
10
10
Sham
TAC3
Sham
TAC3
E
Myh7b
[-fold WT Sham]
Sham
TAC1
TAC3
Sham
TAC1
TAC3
WT
R4496C
F
Nppb
Sham
TAC1
TAC3
Sham
TAC1
TAC3
WT
R4496C
G
cell length/width ratio
213
217
223
242
Sham
TAC1
Sham
TAC1
WT
R4496C

Figure 1

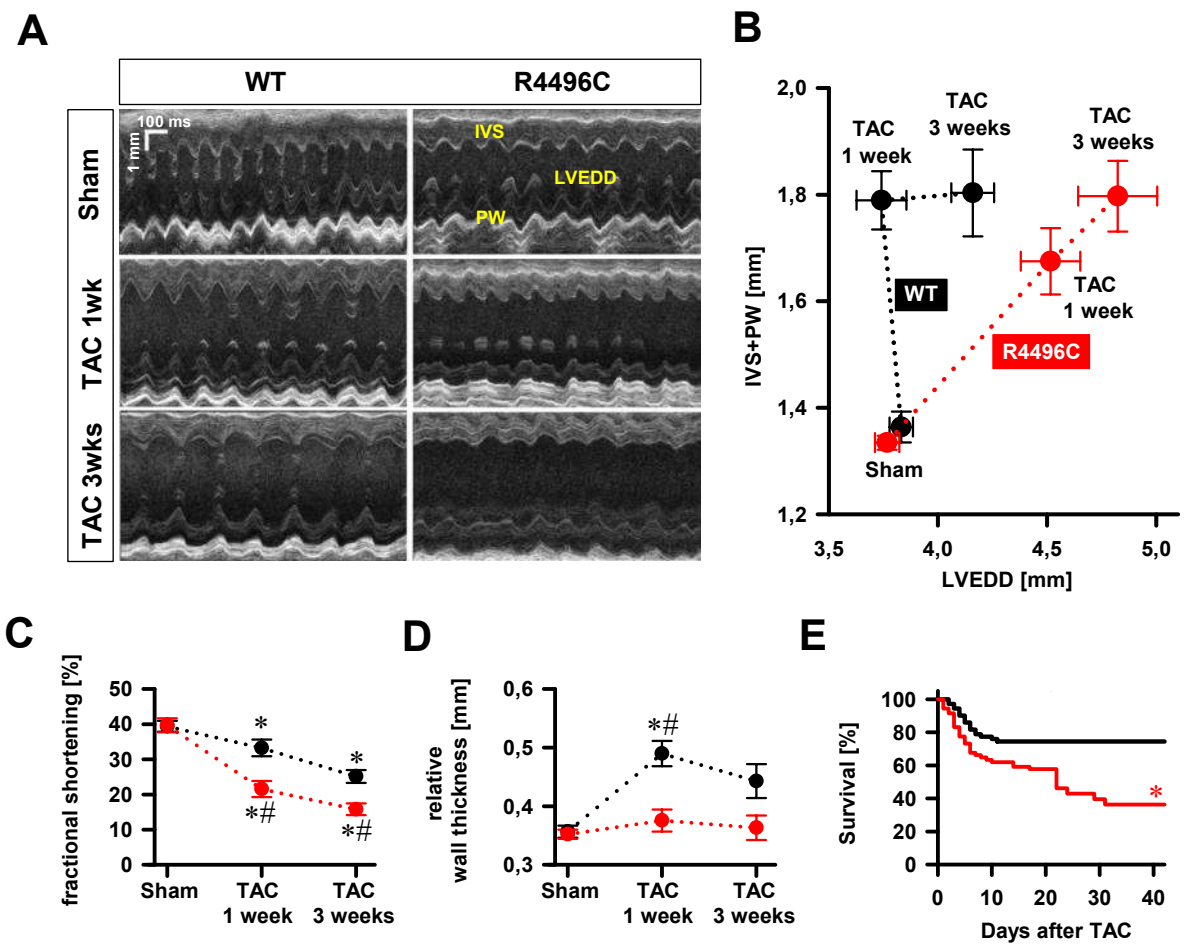
A
WT
R4496C
Sham
TAC 1wk
TAC 3wks
100 ms
1 mm
IVS
LVEDD
PW
B
IVS+PW [mm]
LVEDD [mm]
TAC 1 week
TAC 3 weeks
TAC 3 weeks
TAC 1 week
WT
R4496C
Sham
C
fractional shortening [%]
Sham
TAC 1 week
TAC 3 weeks
D
relative wall thickness [mm]
Sham
TAC 1 week
TAC 3 weeks
E
Survival [%]
Days after TAC

Figure 2

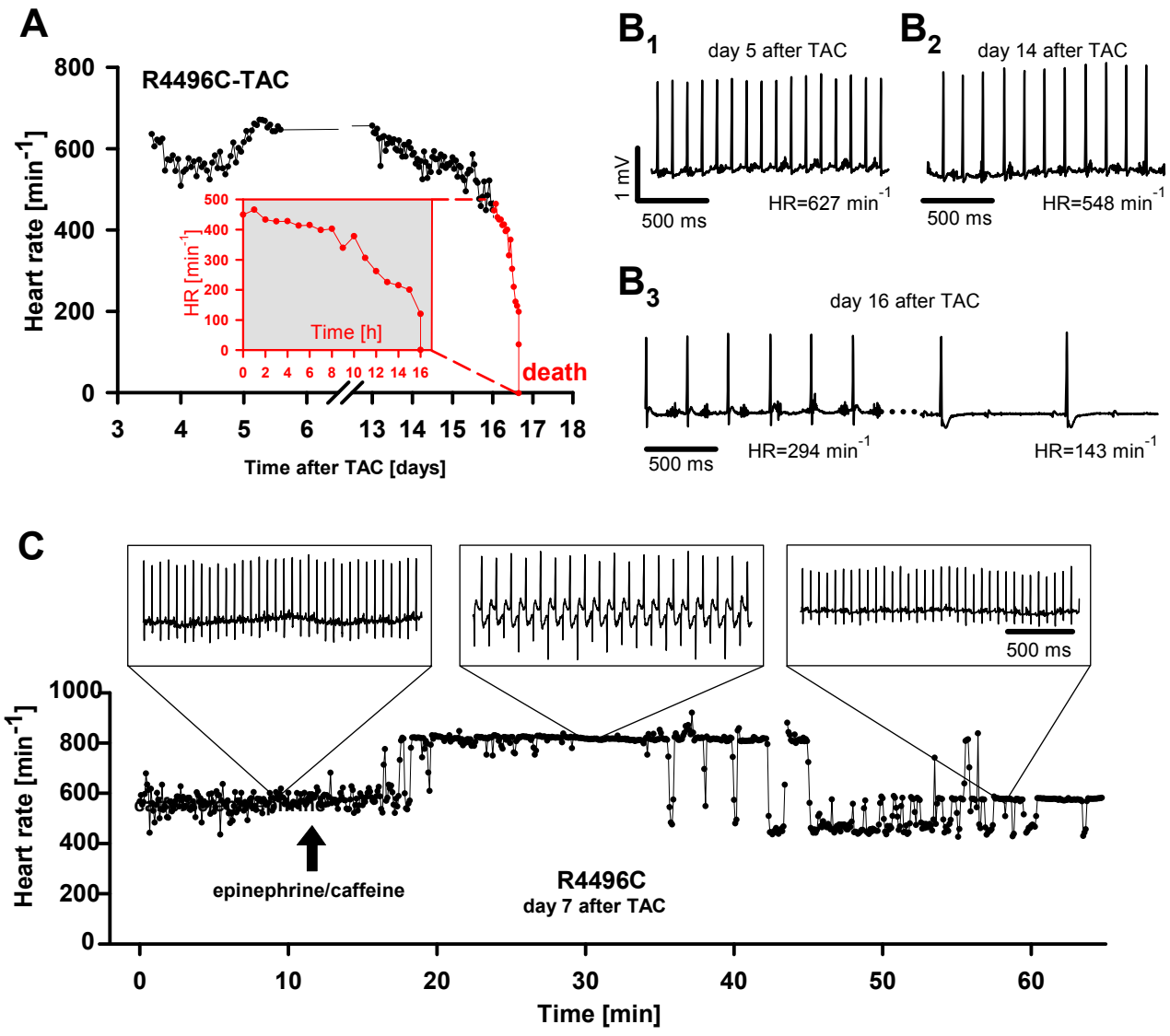
A
R4496C-TAC
Heart rate [min-1]
Time after TAC [days]
HR [min-1]
Time [h]
death
B1
day 5 after TAC
1 mV
500 ms
HR=627 min-1
B2
day 14 after TAC
500 ms
HR=548 min-1
B3
day 16 after TAC
500 ms
HR=294 min-1
HR=143 min-1
C
500 ms
Heart rate [min-1]
epinephrine/caffeine
R4496C
day 7 after TAC
Time [min]

Figure 3

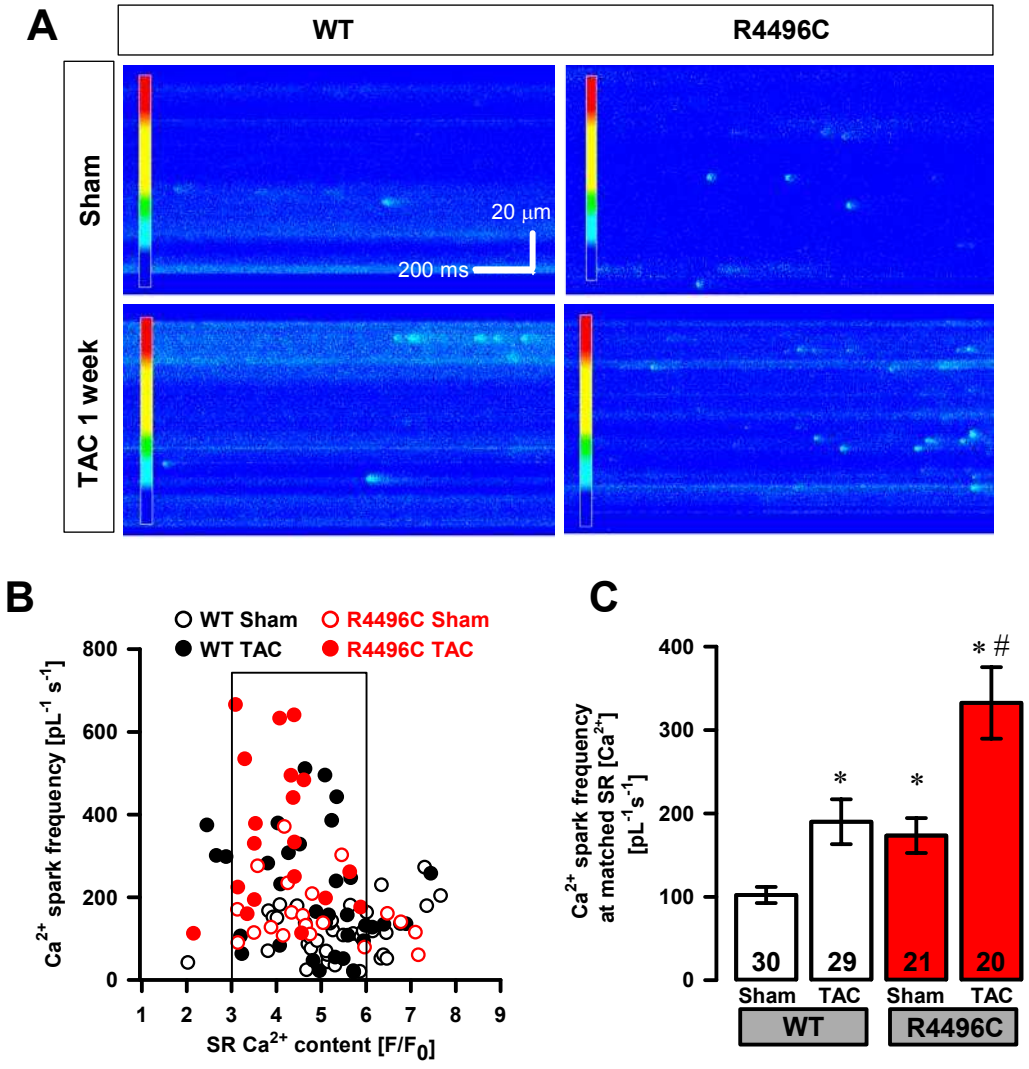
A
WT
R4496C
Sham
TAC 1 week
20 μm
200 ms
B
WT Sham
R4496C Sham
WT TAC
R4496C TAC
Ca2+ spark frequency [pL-1 s-1]
SR Ca2+ content [F/F0]
C
Ca2+ spark frequency at matched SR [Ca2+] [pL-1s-1]
30
29
21
20
Sham
TAC
Sham
TAC
WT
R4496C

Figure 4

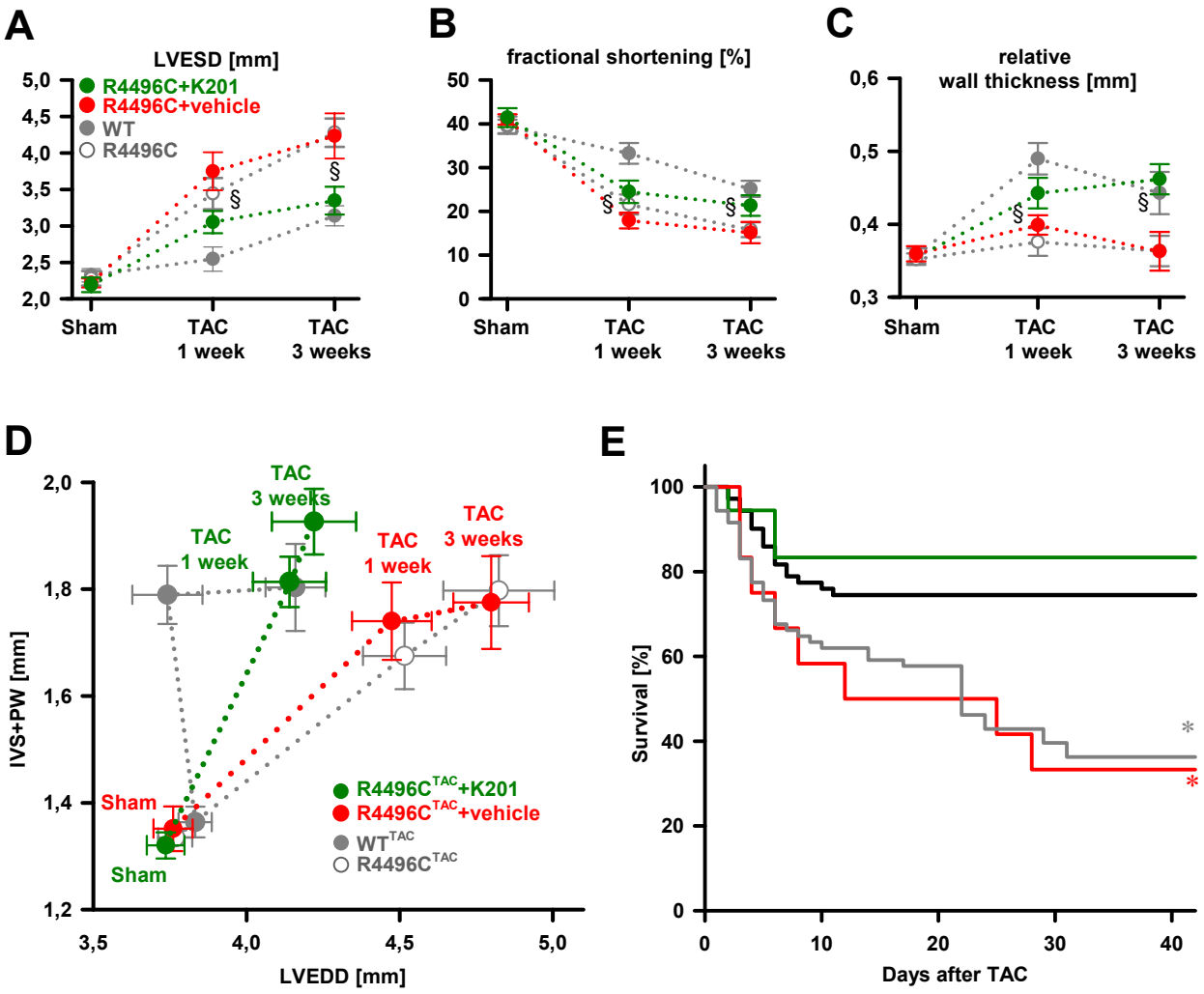
A
LVESD [mm]
R4496C+K201
R4496C+vehicle
WT
R4496C
5,0
4,5
4,0
3,5
3,0
2,5
2,0
Sham
TAC 1 week
TAC 3 weeks
§
B
fractional shortening [%]
50
40
30
20
10
0
C
relative wall thickness [mm]
0,6
0,5
0,4
0,3
D
IVS+PW [mm]
LVEDD [mm]
2,0
1,8
1,6
1,4
1,2
3,5
4,0
4,5
5,0
TAC 3 weeks
TAC 1 week
Sham
R4496C^TAC+K201
R4496C^TAC+vehicle
WT^TAC
R4496C^TAC
E
Survival [%]
100
80
60
40
20
0
10
20
30
40
Days after TAC
*

Figure 7

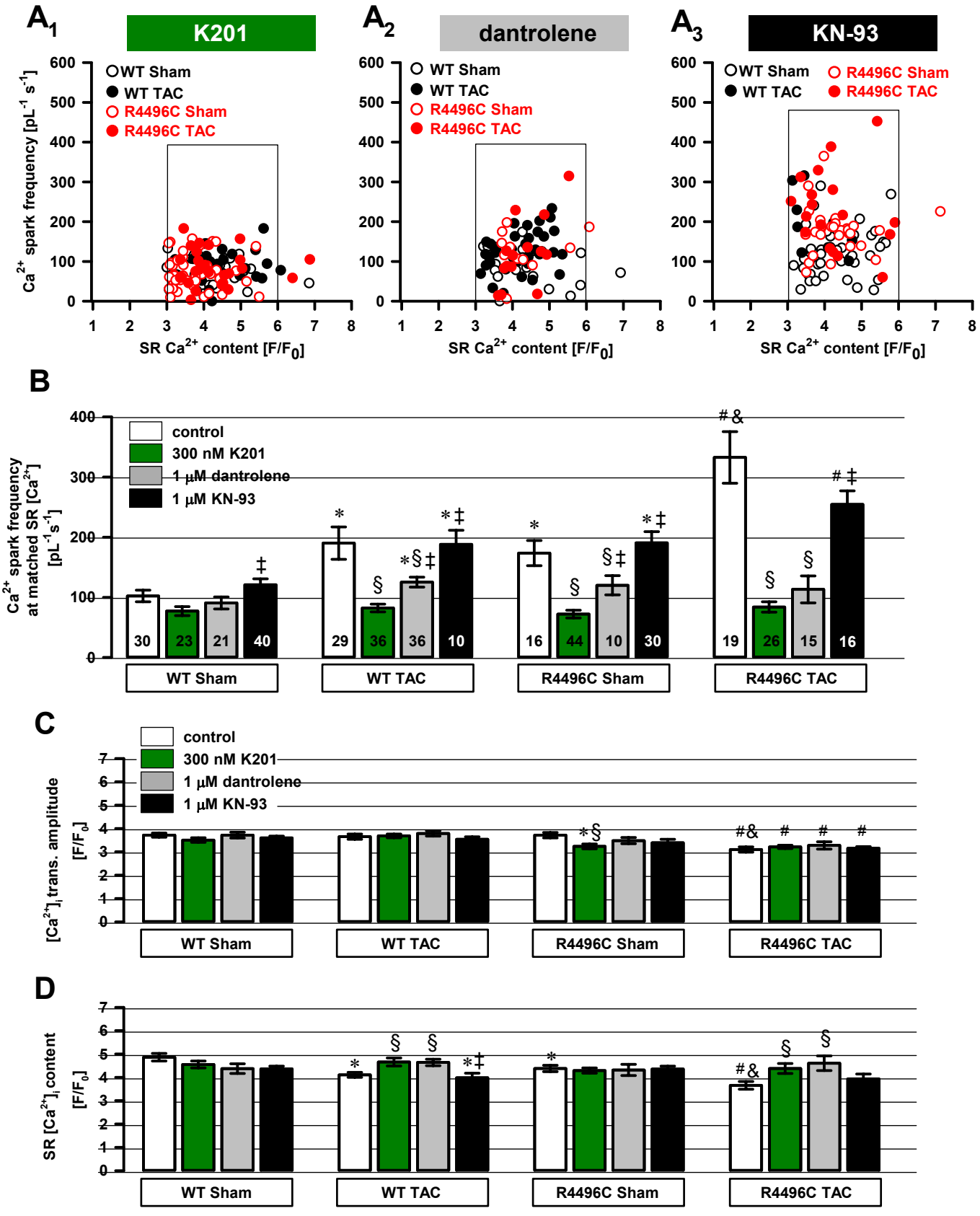
A1
K201
A2
dantrolene
A3
KN-93
WT Sham
WT TAC
R4496C Sham
R4496C TAC
Ca2+ spark frequency [pL-1 s-1]
SR Ca2+ content [F/F0]
B
control
300 nM K201
1 μM dantrolene
1 μM KN-93
Ca2+ spark frequency at matched SR [Ca2+] [pL-1s-1]
30
23
21
40
29
36
36
10
16
44
10
30
19
26
15
16
C
[Ca2+]i trans. amplitude [F/F0]
D
SR [Ca2+]i content [F/F0]

Figure 8

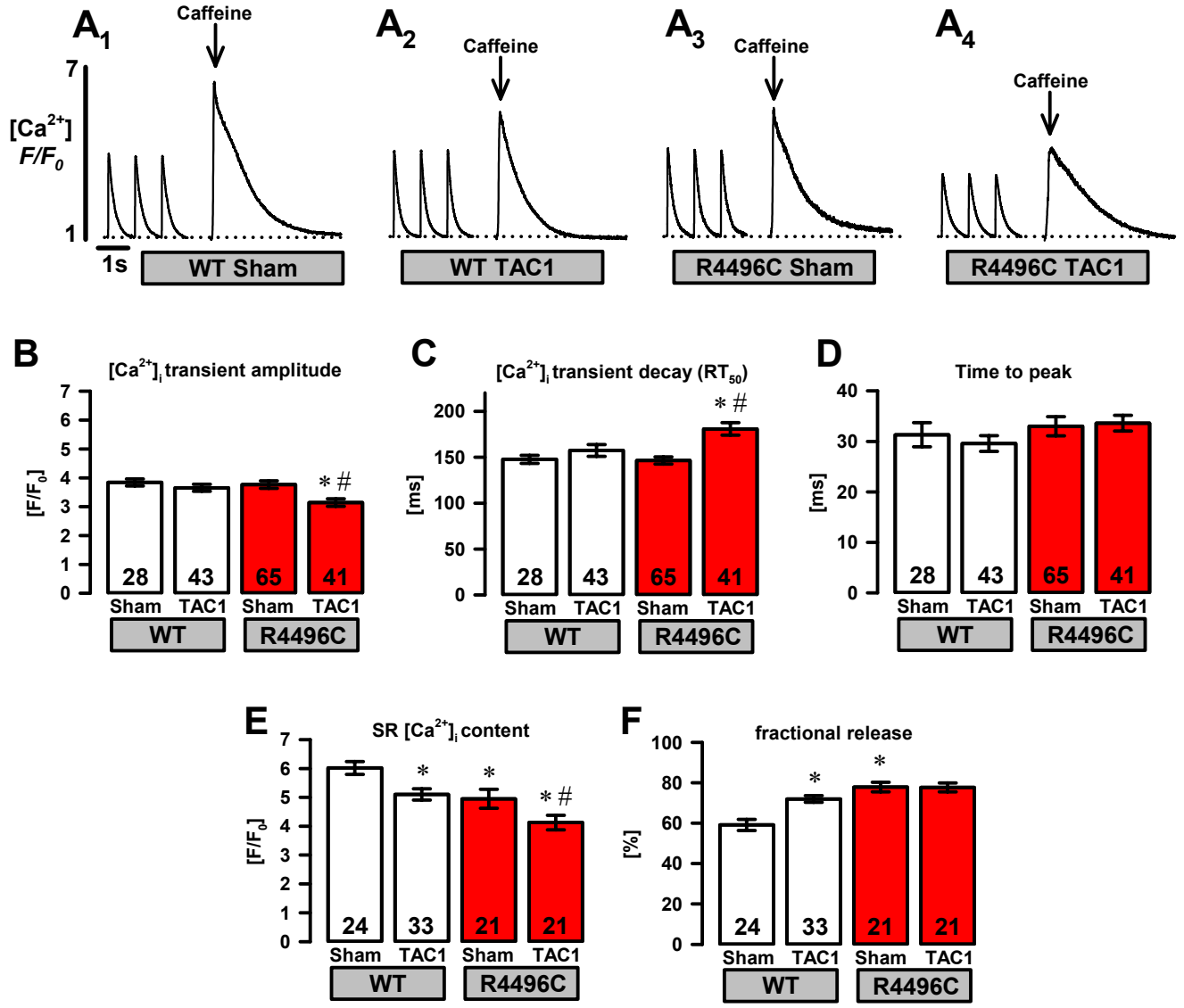
A1
Caffeine
7
[Ca2+]
F/F0
1
1s
WT Sham
A2
Caffeine
WT TAC1
A3
Caffeine
R4496C Sham
A4
Caffeine
R4496C TAC1
B
[Ca2+]i transient amplitude
[F/F0]
28
43
65
41
Sham
TAC1
Sham
TAC1
WT
R4496C
C
[Ca2+]i transient decay (RT50)
[ms]
D
Time to peak
[ms]
E
SR [Ca2+]i content
[F/F0]
24
33
21
21
F
fractional release
[%]

Figure 5

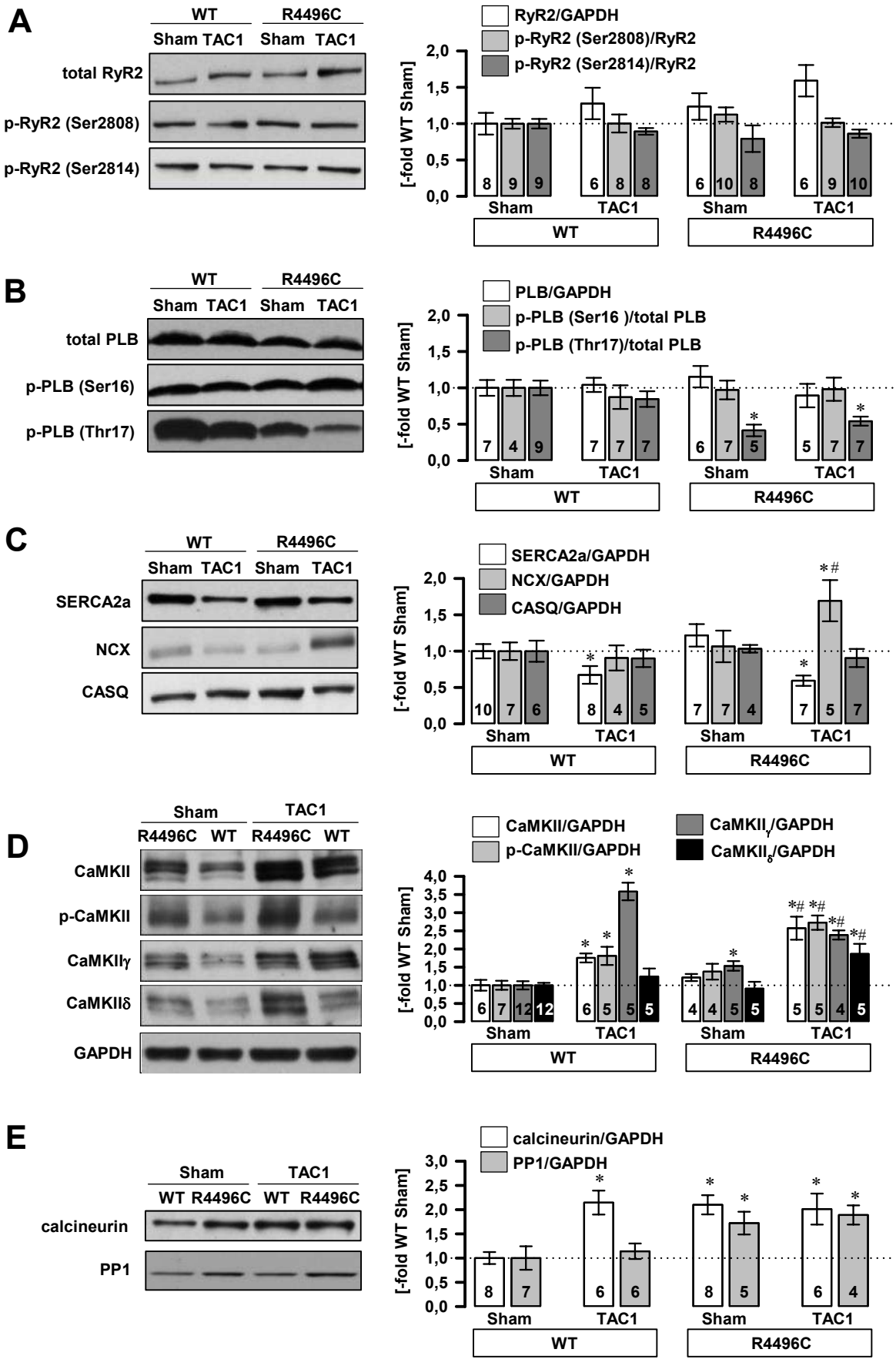
A
WT
R4496C
Sham TAC1 Sham TAC1
total RyR2
p-RyR2 (Ser2808)
p-RyR2 (Ser2814)
RyR2/GAPDH
p-RyR2 (Ser2808)/RyR2
p-RyR2 (Ser2814)/RyR2
[-fold WT Sham]
2,0
1,5
1,0
0,5
0,0
8 9 9 6 8 8 6 10 8 6 9 10
Sham TAC1 Sham TAC1
WT
R4496C
B
WT
R4496C
Sham TAC1 Sham TAC1
total PLB
p-PLB (Ser16)
p-PLB (Thr17)
PLB/GAPDH
p-PLB (Ser16)/total PLB
p-PLB (Thr17)/total PLB
[-fold WT Sham]
2,0
1,5
1,0
0,5
0,0
7 4 9 7 7 7 6 7 5 5 7 7
Sham TAC1 Sham TAC1
WT
R4496C
C
WT
R4496C
Sham TAC1 Sham TAC1
SERCA2a
NCX
CASQ
SERCA2a/GAPDH
NCX/GAPDH
CASQ/GAPDH
[-fold WT Sham]
2,0
1,5
1,0
0,5
0,0
10 7 6 8 4 5 7 7 4 7 5 7
Sham TAC1 Sham TAC1
WT
R4496C
D
Sham
TAC1
R4496C WT R4496C WT
CaMKII
p-CaMKII
CaMKIIγ
CaMKIIδ
GAPDH
CaMKII/GAPDH
p-CaMKII/GAPDH
CaMKIIγ/GAPDH
CaMKIIδ/GAPDH
[-fold WT Sham]
4,0
3,5
3,0
2,5
2,0
1,5
1,0
0,5
0,0
6 7 12 12 6 5 5 5 4 4 5 5 5 5 4 5
Sham TAC1 Sham TAC1
WT
R4496C
E
Sham
TAC1
WT R4496C WT R4496C
calcineurin
PP1
calcineurin/GAPDH
PP1/GAPDH
[-fold WT Sham]
3,0
2,5
2,0
1,5
1,0
0,5
0,0
8 7 6 6 8 5 6 4
Sham TAC1 Sham TAC1
WT
R4496C

Figure 6